

August 2016

# Probing the MSSM explanation of the muon $g-2$ anomaly in dark matter experiments and at a 100 TeV $pp$ collider

Archil Kobakhidze<sup>1</sup>, Matthew Talia<sup>1</sup> and Lei Wu<sup>1,2</sup>

<sup>1</sup> *ARC Centre of Excellence for Particle Physics at the Terascale,  
School of Physics, The University of Sydney, NSW 2006, Australia*

<sup>2</sup> *Department of Physics and Institute of Theoretical Physics, Nanjing Normal University,  
Nanjing, Jiangsu 210023, China*

*E-mails: archil.kobakhidze, matthew.talia, lei.wu1@sydney.edu.au*

## Abstract

We investigate the prospect of current and future dark matter and collider experiments in probing anomalous magnetic moment of the muon,  $(g-2)_\mu$ , within the Minimal Supersymmetric Standard Model (MSSM). Imposing constraints from currently available Higgs data, dark matter relic density, PandaX-II/LUX-2016 experiments and LHC searches for dilepton and tripleton events, we find a range of MSSM parameters with the lightest neutralino  $m_{\tilde{\chi}_1^0} < 800$  GeV and the lightest chargino  $m_{\tilde{\chi}_1^\pm} < 940$  GeV which can accommodate the measured value of  $(g-2)_\mu$  within  $2\sigma$  range. We also observe that a large portion of this parameter space cannot fully account for the observed dark matter abundance (within  $3\sigma$  range) and additional dark matter components beyond MSSM are presumably needed. Further to this we demonstrate that the most of the currently allowed parameter space (except for the compressed region) can be fully probed via searches for tripleton events at a 100 TeV  $pp$  collider.

# 1 Introduction

The discovery of Higgs boson [1, 2] and subsequent measurements of its properties completed the Standard Model (SM) and provided with a very convincing evidence for the simplest perturbative realisation of the electroweak symmetry breaking (EWSB). Despite this overwhelming empirical success, our understanding of EWSB is incomplete. Namely, the quantum corrections are known to drive the Higgs mass (and hence the electroweak scale) towards high-energy scales and thus SM requires unnaturally precise fine-tuning of parameters to satisfy the observations. In addition, observations of neutrino oscillations and dark matter (DM) certainly require beyond the standard model (BSM) physics.

Another deviation from the SM prediction are long seen in the measurements of the the anomalous magnetic moment of the muon,  $a_\mu = (g - 2)_\mu/2$  [3–6]. The recently measured value,

$$\Delta a_\mu^{\text{Exp-SM}} = \begin{cases} (28.7 \pm 8.0) \times 10^{-10} [8], \\ (26.1 \pm 8.0) \times 10^{-10} [9], \end{cases} \quad (1)$$

are more than  $3\sigma$  away from the SM prediction, which includes improved QED [10] and electroweak [11] contributions. Further theoretical progress in calculating QED [12–17] and hadronic contributions [18–27] has also been reported recently. The upcoming experiments at NBL will measure the  $(g - 2)_\mu$  with a precision of 0.14 ppm [28], which would potentially allow to claim  $5\sigma$  discovery of new physics through such measurements. Needless to say, there are several candidate explanations for  $(g - 2)_\mu$  anomaly proposed proposed within various new physics frameworks.

The weak-scale supersymmetry (SUSY) has long been the dominant paradigm for new particle physics. The minimal supersymmetric standard model (MSSM) not only provides an elegant solution to the hierarchy problem but also may successfully explain  $(g - 2)_\mu$  anomaly [29–61]. In MSSM the most significant contribution to  $a_\mu$  is due to the one-loop diagrams involving smuon  $\tilde{\mu}$ , muon sneutrino  $\tilde{\nu}_\mu$ , neutralinos  $\tilde{\chi}^0$  and charginos  $\tilde{\chi}^\pm$ . The one-loop contribution to  $a_\mu$  arises if there is a chirality flip between incoming and outgoing external muon lines, which may be induced through the  $L - R$  mixing in the smuon sector or the SUSY Yukawa couplings of Higgsinos to muon and  $\tilde{\mu}$  or  $\tilde{\nu}_\mu$ . Therefore, these contributions to  $a_\mu$  are typically proportional to  $m_\mu^2/M_{SUSY}^2$ . Thus, to generate the sizable contributions to  $a_\mu$ , the SUSY scale  $M_{SUSY}$  encapsulating slepton and electroweakino masses has to be around  $O(100)$  GeV. So, the detection of light sleptons and electroweakinos will provide a test for the MSSM solution to the  $(g - 2)_\mu$  problem.

The negative results of direct searches for sparticles during the LHC Run-1 have pushed up the mass limits of the first two generation squarks and gluino into the TeV region [62, 63]. The third generation squarks have been tightly constrained in the simplified models [64, 65], such as in Stealth SUSY [66] and Natural SUSY [67–69]. Unlike the colored sparticles, the bounds on the sleptons [70, 71] and electroweakinos [72, 73]

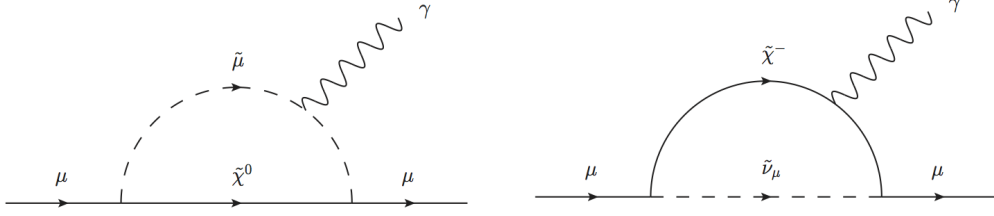


Figure 1: One-loop diagram contributions of the MSSM to the muon anomalous magnetic moment,  $(g - 2)_\mu$ . The first involves a smuon-neutralino (left) and the second a chargino-muon sneutrino loop (right).

are relatively weak, especially for the region of compressed spectrum. The lightest neutralino still remains as a successful dark matter (DM) candidate and significant effort has been made to obtain a lower mass limit on the neutralino LSP in MSSM, see e.g. [74–78].

In this paper, we explore potential of the current and future dark matter and collider experiments to probe anomalous magnetic moment of the muon within MSSM. Using the LEP and Higgs data and demanding that the theory accommodates  $(g - 2)_\mu$  measurements within  $2\sigma$  range, we derive bounds on the electroweakino masses. Following this, we impose dark matter constraints from Planck, PandaX-II/LUX 2016 data and constraints from LHC searches for dilepton and trilepton events (Sec. 3). Finally, we evaluate the prospect of a future 100 TeV hadron collider in probing electroweakinos in trilepton events within this scenario (Sec. 4). Our conclusions are presented in Sec. 5.

## 2 $(g - 2)_\mu$ in MSSM

The low-energy effective operator for magnetic dipole moment (MDM) is given by:

$$\mathcal{L}_{MDM} = \frac{e}{4m_\mu} a_\mu \bar{\mu} \sigma_{\rho\lambda} \mu F^{\rho\lambda}. \quad (2)$$

where  $e$  is the electric charge and  $m_\mu$  is the muon mass.  $F^{\rho\lambda}$  is the field strength of the photon field and  $\sigma_{\rho\lambda} = \frac{i}{2} [\gamma_\rho, \gamma_\lambda]$ .

In MSSM, there are essentially two types of diagrams which contribute to  $a_\mu$  at one-loop, i.e. one is the  $\tilde{\chi}^0 - \tilde{\mu}$  loop diagram (left panel of Fig. 1) and the other is the chargino  $\tilde{\chi}^\pm - \tilde{\nu}_\mu$  loop diagram (right panel of Fig. 1). The expressions for one-loop SUSY corrections to  $a_\mu$  (including the complex phases effects) are given by [31]

$$a_\mu^{\tilde{\chi}^0} = \frac{m_\mu}{16\pi^2} \sum_{i,\alpha} \left\{ -\frac{m_\mu}{12m_{\tilde{\mu}_m}^2} (|n_{i\alpha}^L|^2 + |n_{i\alpha}^R|^2) F_1^N(x_{i\alpha}) + \frac{m_{\tilde{\chi}_i^0}}{3m_{\tilde{\mu}_m}^2} \text{Re}(n_{i\alpha}^L n_{i\alpha}^R) F_2^N(x_{i\alpha}) \right\} \quad (3)$$

$$a_\mu^{\tilde{\chi}^\pm} = \frac{m_\mu}{16\pi^2} \sum_j \left\{ \frac{m_\mu}{12m_{\tilde{\nu}_\mu}^2} (|c_j^L|^2 + |c_j^R|^2) F_1^C(x_j) + \frac{2m_{\tilde{\chi}_j^\pm}}{3m_{\tilde{\nu}_\mu}^2} \text{Re}(c_j^L c_j^R) F_2^C(x_j) \right\} \quad (4)$$

where  $i = 1, 2, 3, 4$ ,  $j = 1, 2$  and  $\alpha = 1, 2$  denotes the neutralino, chargino and smuon mass eigenstates, respectively. The couplings are defined as

$$\begin{aligned} n_{i\alpha}^R &= \sqrt{2}g_1 N_{i1} X_{\alpha 2} + y_\mu N_{i3} X_{\alpha 1}, \\ n_{i\alpha}^L &= \frac{1}{\sqrt{2}}(g_2 N_{i2} + g_1 N_{i1}) X_{\alpha 1}^* - y_\mu N_{i3} X_{\alpha 2}^*, \\ c_j^R &= y_\mu U_{j2}, \\ c_j^L &= -g_2 V_{j1}, \end{aligned} \tag{5}$$

where the muon Yukawa coupling  $y_\mu = g_2 m_\mu / \sqrt{2} m_W \cos \beta$ .  $N$  are the neutralino and  $U, V$  are the chargino mixing matrices, respectively.  $X$  denotes the slepton mixing matrix. In terms of the kinematic variables  $x_{i\alpha} = m_{\tilde{\chi}_i^0}^2 / m_{\tilde{\mu}_\alpha}^2$  and  $x_j = m_{\tilde{\chi}_j^\pm}^2 / m_{\tilde{\nu}_\mu}^2$ , the loop functions  $F$  are defined as follows

$$\begin{aligned} F_1^N(x) &= \frac{2}{(1-x)^4} \left[ 1 - 6x + 3x^2 + 2x^3 - 6x^2 \ln x \right], \\ F_2^N(x) &= \frac{3}{(1-x)^3} \left[ 1 - x^2 + 2x \ln x \right], \\ F_1^C(x) &= \frac{2}{(1-x)^4} \left[ 2 + 3x - 6x^2 + x^3 + 6x \ln x \right], \\ F_2^C(x) &= -\frac{3}{2(1-x)^3} \left[ 3 - 4x + x^2 + 2 \ln x \right]. \end{aligned} \tag{6}$$

These one-loop corrections mainly rely on the bino/wino masses  $M_{1,2}$ , the Higgsino mass  $\mu$ , the left- and right-smuon mass parameters,  $M_{\tilde{\mu}_L, \tilde{\mu}_R}$ , and the ratio of the two Higgs vacuum expectation values,  $\tan \beta$ . They have a weak dependence on the second generation trilinear coupling  $A_\mu$ . In the limit of large  $\tan \beta$ , when all the mass scales are roughly of the same order of  $M_{SUSY}$ , the contributions Eq. (3) and Eq. (4) can be approximately written as

$$a_\mu^{\tilde{\chi}^\pm} \simeq \frac{m_\mu^2 g_2^2}{32\pi^2 M_{SUSY}^2} \tan \beta; \tag{7}$$

$$a_\mu^{\tilde{\chi}^0} \simeq \frac{m_\mu^2}{192\pi^2 M_{SUSY}^2} (g_1^2 - g_2^2) \tan \beta. \tag{8}$$

The detailed dependence of  $a_\mu$  on the five relevant mass parameters  $\tan \beta$  is complicated. For two-loop corrections, it should be noted that if the squark masses (or masses of the first or third generation slepton) become large, the SUSY contributions to  $a_\mu$  do not decouple but are logarithmically enhanced. Depending on the mass pattern, a positive or negative correction of O(10%) for squark masses in the few TeV region can be obtained, see Ref. [79].

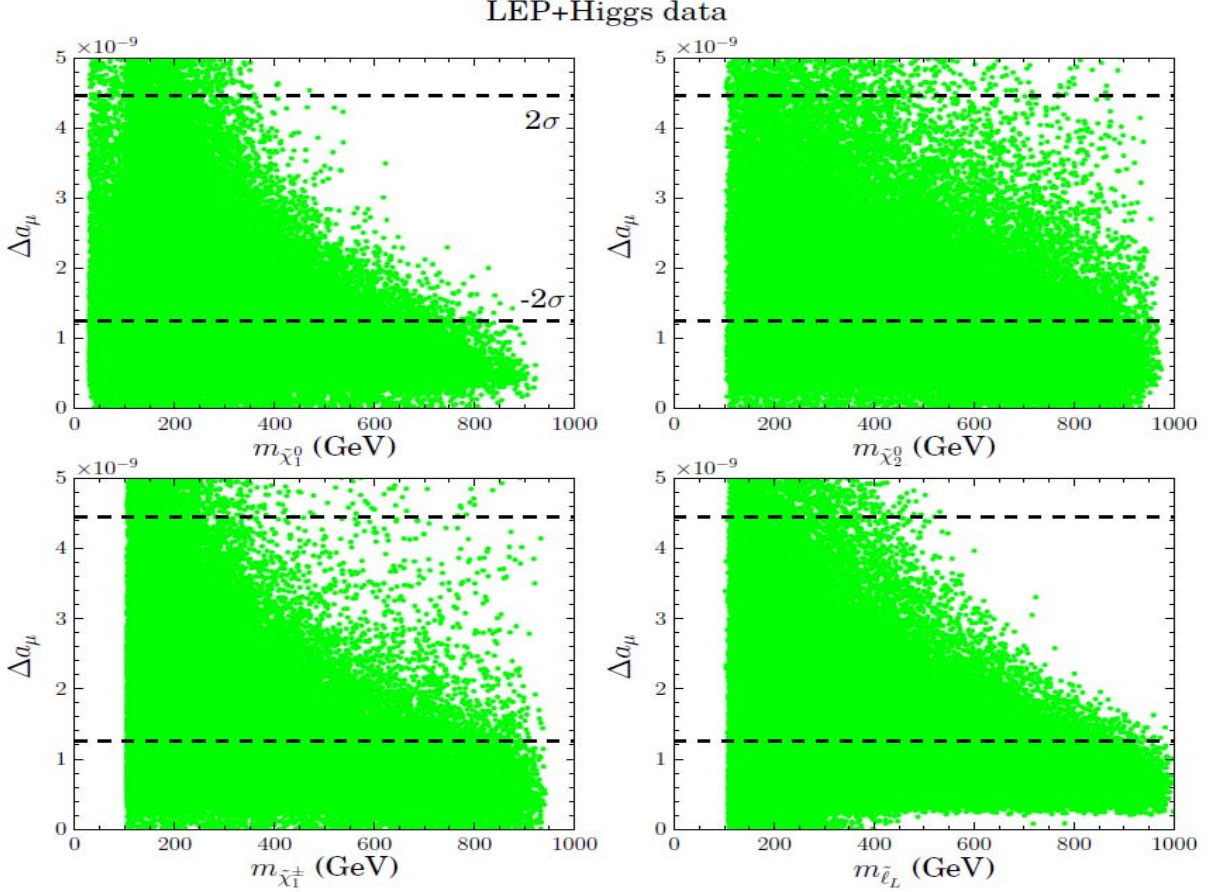


Figure 2: Scatter plot on the plane of  $\Delta a_\mu$  and sparticle masses. Green circles satisfy the constraints from LEP and LHC Higgs data. The dashed lines represent the  $2\sigma$  band on  $\Delta a_\mu$  given by Eq.(1).

### 3 Constraints on MSSM Explanation of $(g - 2)_\mu$

In the following, we numerically calculate  $a_\mu$  by using the **FeynHiggs-2.11.2** [80] package and scan the relevant MSSM parameter space:

$$10 < \tan \beta < 50, \quad -1 \text{ TeV} < M_1, M_2, \mu < 1 \text{ TeV}, \quad 0.1 \text{ TeV} < m_{\tilde{t}_L}, m_{\tilde{t}_R} < 1 \text{ TeV} \quad (9)$$

where we have the subscript  $\ell = e, \mu$ . Due to the small effects on  $a_\mu$ , the slepton trilinear parameters of the first two generation are assumed as  $A_\ell = 0$ . To satisfy the 125 GeV Higgs mass within a 2 GeV deviation, we vary the stop trilinear parameter in the range  $|A_t| < 5 \text{ TeV}$  and set the stop soft masses at 5 TeV. We require the mixing parameter  $|X_t/M_S| < 2$  to avoid the charge/colour-breaking minima [81]. We calculate the Higgs mass with **FeynHiggs-2.12.2** [80]. In our scan, we also consider the following experimental bounds:

- LEP: the direct searches for the slepton and chargino at LEP produce the lower

mass limits on the first two generation sleptons and lightest chargino [82]:

$$m_{\tilde{l}_L}, m_{\tilde{l}_R} > 100 \text{ GeV} \quad (l = e, \mu) \quad (10)$$

$$m_{\tilde{\chi}_1^\pm} > 105 \text{ GeV} \quad (11)$$

- Higgs data: the exclusion limits at 95% CL from the experimental cross sections from higgs searches at LEP, Tevatron and LHC are examined by using HiggsBounds-4.2.1 [83].
- We require the lightest neutralino  $\tilde{\chi}_1^0$  as the LSP and  $m_{\tilde{\chi}_1^0} > 30 \text{ GeV}$  to be consistent with the bound on light MSSM neutralino dark matter [84].

In Fig. 2, we present the dependence of  $\Delta a_\mu$  on the masses of neutralinos ( $\tilde{\chi}_{1,2}^0$ ), charginos ( $\tilde{\chi}_{1,2}^\pm$ ) and smuons ( $\tilde{\mu}_{1,2}$ ). We find that the lighter these sparticles are, the larger  $\Delta a_\mu$  becomes. The explanation of  $\Delta a_\mu$  within a  $2\sigma$  range requires  $m_{\tilde{\chi}_1^0} < 800 \text{ GeV}$ ,  $m_{\tilde{\chi}_1^\pm, \tilde{\chi}_2^0} < 940 \text{ GeV}$  and  $\tilde{\mu}_1 < 930 \text{ GeV}$ . The  $\tilde{\chi}^\pm\text{-}\tilde{\nu}_\mu$  loop dominates over the  $\tilde{\chi}^0\text{-}\tilde{\mu}$  loop. A sizable SUSY contribution to  $a_\mu$  can be obtained, if  $M_1$ ,  $M_2$  and  $\mu$  have the same sign and  $\tilde{\chi}_{1,2}^0$  and  $\tilde{\chi}_1^\pm$  have a sizable higgsino, wino or both components with large  $\tan\beta$ . However, a higgsino or wino-like LSP usually suffers from the constraints of the dark matter relic density and direct detection experiments.

Next, we confront the MSSM explanation of  $(g-2)_\mu$  with the various dark matter experiments. We use MicrOmegas-4.2.3 [85] to calculate the dark matter relic density  $\Omega h^2$  and the spin-independent neutralino scattering cross sections with nuclei, denoted as  $\sigma^{SI}$ . It should be noted that the thermal relic abundance of the light higgsino or wino-like neutralino dark matter is typically low due to the large annihilation rate in the early universe. This leads to the standard thermally produced WIMP dark matter being under-abundant. In order to have the correct relic density, several alternatives have been proposed, such as choosing the axion-higgsino admixture as a dark matter candidate [86]. So we rescale the scattering cross section  $\sigma^{SI}$  by a factor of  $(\Omega h^2 / \Omega_{Planck} h^2)$ , where  $\Omega_{Planck} h^2 = 0.112 \pm 0.006$  is the relic density measured by Planck satellite [87].

In Fig. 3, we show the neutralino dark matter relic density  $\Omega h^2$  (left) and the spin-independent neutralino-nucleon scattering cross section  $\sigma^{SI}$  (right). All samples satisfy the LEP, Higgs data and  $(g-2)_\mu$  within  $2\sigma$ . In the left panel of Fig. 3, it can be seen that there are an amount of samples above the  $3\sigma$  upper bound of the Planck relic density measurement. Those samples are bino-like and annihilate to the SM particles very slowly, which leads to an overabundance of dark matter in the universe. On the other hand, there are two dips around  $M_Z$  and  $M_h$ , respectively, where  $\tilde{\chi}_1^0\tilde{\chi}_1^0$  can efficiently annihilate through the resonance effect. When the LSP higgsino or wino component dominates, the annihilation cross section of  $\tilde{\chi}_1^0\tilde{\chi}_1^0$  is small so that the relic density is less than the  $3\sigma$  lower bound of the Planck value. A mixed LSP with a certain higgsino or wino fraction [88] can be reconciled with the measured relic abundance  $\Omega h^2$  within the  $3\sigma$  range. In the right panel of Fig. 3, we project the samples that satisfy  $3\sigma$

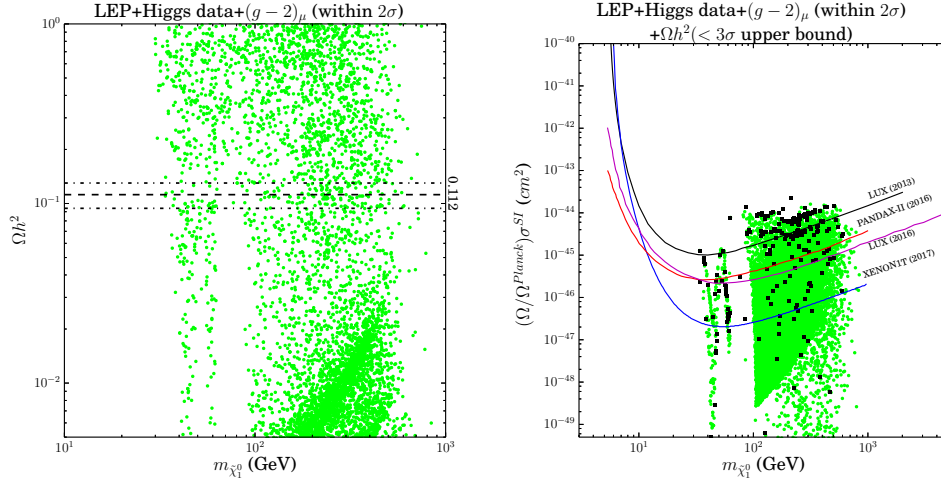


Figure 3: The neutralino dark matter relic density  $\Omega h^2$  (left) and the spin-independent neutralino-nucleon scattering cross section  $\sigma^{SI}$  (right). The dashed line is the PLANCK central value and the dashed-dotted lines are corresponding  $3\sigma$  bands. The exclusion limits on the  $\sigma^{SI}$  from LUX (2013) [89] (black line), LUX (2016) (magenta line) [91], PandaX-II (red line) [90], and XENON1T (2017) projected [92] (blue line). Green circles satisfy the LEP, Higgs data and  $2\sigma$  bound of  $(g-2)_\mu$  (left) and  $3\sigma$  upper bound of  $\Omega h^2$ , while the black squares further require  $\Omega h^2$  within  $3\sigma$  range.

upper bound  $\Omega_{Planck} h^2$  on the plane of  $\sigma^{SI}$  versus  $m_{\tilde{\chi}_1^0}$ . We can see that a large portion of the parameter space with higgsino or wino-like LSP can be excluded by the recent PandaX-II [90] and LUX data [91]. The future XENON1T (2017) experiment [92] can further cover the parameter space, where the LSP has a certain amount of bino component.

Given the great progress of LHC experiments, we recast the results of searching for  $2\ell + \cancel{E}_T$  and  $3\ell + \cancel{E}_T$  signatures at LHC-8 TeV. The main processes contributing to  $2\ell + \cancel{E}_T$  events can arise from the production of sleptons pair and charginos:

$$pp \rightarrow \tilde{\ell}^+ \tilde{\ell}^-, \tilde{\chi}_1^+ \tilde{\chi}_1^- \quad (12)$$

with the subsequent decays to leptons:

- slepton decay:  $\tilde{\ell}^\pm \rightarrow \ell^\pm \tilde{\chi}_1^0$ ;
- chargino decays: (a) through sleptons:  $\tilde{\chi}_1^\pm \rightarrow \tilde{\ell}^\pm (\rightarrow \ell^\pm \tilde{\chi}_1^0) \nu_\ell$ , (b) through sneutrinos:  $\tilde{\chi}_1^\pm \rightarrow \tilde{\nu}_\ell (\rightarrow \nu_\ell \tilde{\chi}_1^0) \ell^\pm$ , (c) through  $W$  boson:  $\tilde{\chi}_1^\pm \rightarrow W^\pm (\rightarrow \ell^\pm \nu_\ell) \tilde{\chi}_1^0$ .

While  $3\ell + \cancel{E}_T$  events mainly come from the associated production of chargino and neutralino:

$$pp \rightarrow \tilde{\chi}_i^0 \tilde{\chi}_j^\pm \quad (13)$$

where  $i = 2, 3, 4$  and  $j = 1, 2$ . They then decay in two different ways:

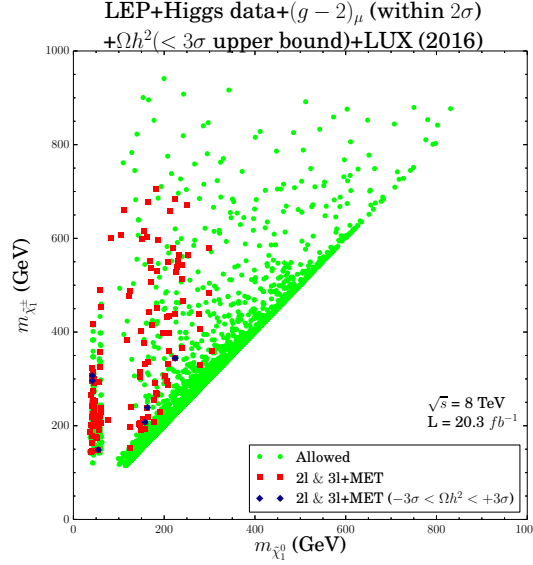


Figure 4: Exclusion limits from LHC Run-1 dilepton and trilepton events. All samples satisfy the LEP, Higgs data,  $3\sigma$  upper bound of the dark matter relic density, LUX 2016 and  $(g-2)_\mu$  within the  $2\sigma$ . Red squares ( $\Omega h^2 < +3\sigma$ ) and blue diamonds ( $-3\sigma < \Omega h^2 < +3\sigma$ ) are excluded by  $2\ell + \cancel{E}_T$  and  $3\ell + \cancel{E}_T$  events.

- through sleptons/sneutrinos: (a)  $\tilde{\chi}_i^0 \rightarrow \ell^\mp \tilde{\ell}^\pm (\rightarrow \ell^\pm \tilde{\chi}_1^0)$ ,  $\tilde{\chi}_j^\pm \rightarrow \tilde{\ell}^\pm (\rightarrow \ell^\pm \tilde{\chi}_1^0) \nu_\ell$ , (b)  $\tilde{\chi}_i^0 \rightarrow \ell^\mp \tilde{\ell}^\pm (\rightarrow \ell^\pm \tilde{\chi}_1^0)$ ,  $\tilde{\chi}_j^\pm \rightarrow \tilde{\nu}_\ell (\rightarrow \nu_\ell \tilde{\chi}_1^0) \ell^\pm$ ;
- through the SM gauge bosons:  $\tilde{\chi}_i^0 \rightarrow Z^{(*)} (\rightarrow \ell^\pm \ell^\mp) \tilde{\chi}_1^0$ ,  $\tilde{\chi}_j^\pm \rightarrow W^{\pm(*)} (\rightarrow \ell^\pm \nu_\ell) \tilde{\chi}_1^0$ .

We use **SPheno-3.3.8** [93] to produce the SLHA file to employ in **MadGraph5\_aMC@NLO** [94] and generate the parton level signal events. Then the events are showered and hadronized by **PYTHIA** [95]. The detector effects are included by using the tuned **Delphes** [96]. **FastJet** [97] is used to cluster jets with the anti- $k_t$  algorithm [98]. We recast the ATLAS dilepton [70] and trilepton [72] analyses<sup>1</sup> by using **CheckMATE-1.2.2** [100]. We include the NLO correction effects in the production of  $\tilde{\ell}^\pm \tilde{\ell}^\mp$ ,  $\tilde{\chi}_i^\pm \tilde{\chi}_i^\mp$  and  $\tilde{\chi}_i^0 \tilde{\chi}_j^\pm$  productions by multiplying a  $K$ -factor 1.3 [101]. The main SM backgrounds include  $WZ$ ,  $ZZ$  and  $t\bar{t}V$  ( $V = W, Z$ ). To estimate the exclusion limit, we define the ratio  $r = \max(N_{S,i}/S_{obs,i}^{95\%})$ , where  $N_{S,i}$  and  $S_{obs,i}^{95\%}$  are the event numbers of the signal for  $i$ -th signal region and the corresponding observed 95% C.L. upper limit, respectively. The max is over all signal regions defined in the analysis. We conclude that a sample is excluded at 95% C.L., if  $r > 1$ .

<sup>1</sup>Very recently, the CMS collaboration updated the results of search for electroweak SUSY production in multilepton final states in  $12.9 \text{ fb}^{-1}$  data at  $\sqrt{s} = 13 \text{ TeV}$  [99]. Based on certain assumptions on slepton mass and  $\tilde{\chi}_2^0 \rightarrow \ell\bar{\ell}$  branching fraction, the exclusion limits are improved by 100 GeV–300 GeV. It is reasonable to expect that the current 13 TeV data can further exclude a portion of samples, but still can not cover majority of the allowed samples in the entire mass range.



In Fig. 4, we recast the LHC Run-1 dilepton and trilepton exclusion limits on the plane of  $m_{\tilde{\chi}_1^\pm}$  and  $m_{\tilde{\chi}_1^0}$ . All samples satisfy the LEP, Higgs data,  $3\sigma$  upper bound of relic density, LUX 2016 and  $(g-2)_\mu$  within  $2\sigma$  range. Red squares ( $\Omega h^2 < +3\sigma$ ) and blue diamonds ( $-3\sigma < \Omega h^2 < +3\sigma$ ) are excluded by  $2\ell + \cancel{E}_T$  and  $3\ell + \cancel{E}_T$  events. In Fig. 4, we can see that a portion of samples in  $\tilde{\chi}_1^\pm < 710$  GeV and  $\tilde{\chi}_1^0 < 300$  GeV can be excluded. A bulk of samples in the parameter space with  $\tilde{\chi}_1^\pm$  being higgsino or wino-like can not be covered because of the small mass difference between  $\tilde{\chi}_1^\pm$  and  $\tilde{\chi}_1^0$ . Such a region may be accessed by the monojet(-like) or the VBF production at HL-LHC [102–108]. In addition, when  $\tilde{\chi}_2^0$  has a sizable bino component, the limit from trilepton events will become weak because of the reduction of cross section of  $\tilde{\chi}_1^\pm \tilde{\chi}_2^0$ . We also find that the dilepton channel can be complimentary to the trilepton channel when the latter is suppressed by small neutralino leptonic branching ratios. An important factor in the dilepton and trilepton yields is the leptonic branching fraction which can vary widely throughout the parameter space. If the slepton is on shell, the chargino two-body decays then dominate and its leptonic branching fraction is maximized,  $Br(\tilde{\chi}_1^\pm \rightarrow \tilde{\chi}_1^0 \tilde{\ell}^\pm (\rightarrow \ell^\pm \nu_\ell))_{max} = 2/3$ . When the sneutrino is on-shell and is lighter than the corresponding slepton, the channel  $\tilde{\chi}_2^0 \rightarrow \nu_\ell \tilde{\nu}_\ell$  will dominate the decay width, and the neutralino leptonic branching ratio is suppressed. On the other hand, if the slepton and sneutrino are heavy enough, the decay amplitudes of  $\tilde{\chi}_1^\pm$  and  $\tilde{\chi}_2^0$  are dominated by  $W$  and  $Z$  boson exchange, respectively, which give  $\tilde{\chi}_1^\pm \rightarrow \tilde{\chi}_1^0 W^\pm (\rightarrow \ell^\pm \nu_\ell) \simeq 2/9$  and  $\tilde{\chi}_2^0 \rightarrow \tilde{\chi}_1^0 Z (\rightarrow \ell^\pm \ell^\mp) \simeq 6\%$ . On the other hand,  $\tilde{\chi}_2^0$  can decay to  $h\tilde{\chi}_1^0$  with a sizable branching ratio if kinematically accessible, which can also weaken the trilepton exclusion limit.

## 4 Prospects at a 100 TeV Collider

To hunt for new fundamental particles, a 100 TeV  $pp$  collider has been under discussion in recent years, which will allow us to probe the new physics scale roughly an order of magnitude higher than we can possibly reach with the LHC [109]. Several studies of electroweakinos and sleptons at an 100 TeV  $pp$  collider have been carried out in the recent past [110–115]. In this section, we estimate the prospects of probing the MSSM explanation of the  $(g-2)_\mu$  anomaly by extrapolating the above 8 TeV trilepton analysis to a 100 TeV  $pp$  collider. For each allowed sample above, we use the most sensitive signal region in 8 TeV analysis and simply assume the same detection efficiency in 100 TeV analysis. We rescale the signal ( $S$ ) and background ( $B$ ) events by the following ratio:

$$N^{100\text{ TeV}} = (\sigma^{100\text{ TeV}}/\sigma^{8\text{ TeV}})(3000\text{ fb}^{-1}/20.3\text{ fb}^{-1})N^{8\text{ TeV}} \quad (14)$$

Such a treatment can be considered as a preliminary theoretical estimation. The optimized analysis strategy may be achieved once the details of the collider environment

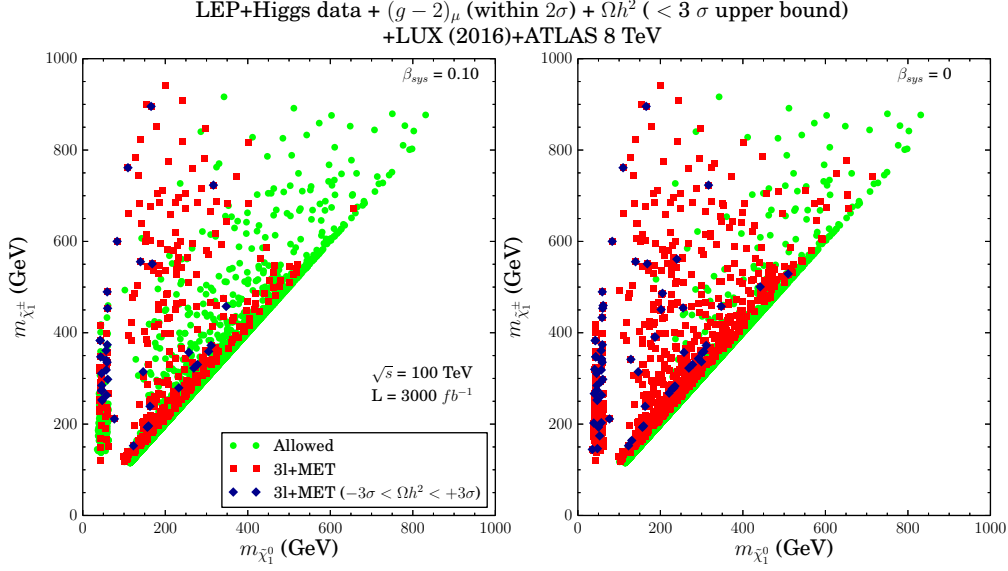


Figure 5: Same as Fig. 4, but for expected exclusion limit at a 100 TeV  $pp$  collider with the luminosity of  $3000 \text{ fb}^{-1}$ . Red squares ( $\Omega h^2 < +3\sigma$ ) and blue diamonds  $-3\sigma < \Omega h^2 < +3\sigma$  are excluded by searching for  $3\ell + \text{MET}$  events. The systematic uncertainty  $\beta_{sys}$  is taken as 0.1 and 0, respectively.

is known. To obtain the expected exclusion limits, we use the following equation,

$$\frac{S}{\sqrt{B + (\beta_{sys}B)^2}} \geq 2 \quad [\text{Excluded}] \quad (15)$$

where the factor  $\beta_{sys}$  parameterizes the systematic uncertainty. In Fig. 4, we can see that when  $\beta_{sys} = 0.1$ , a majority of samples allowed by  $(g-2)_\mu$  in the parameter space with  $\tilde{\chi}_1^0 < 530 \text{ GeV}$  and  $\tilde{\chi}_1^\pm < 940 \text{ GeV}$  can be excluded. Such a range will be extended to  $\tilde{\chi}_1^0 < 710 \text{ GeV}$  and  $\tilde{\chi}_1^\pm < 940 \text{ GeV}$ , if  $\beta_{sys} = 0$ . Almost all our samples that satisfy the dark matter relic density within  $3\sigma$  range can be covered. Again, the compressed region of  $\tilde{\chi}_1^\pm$  and  $\tilde{\chi}_1^0$  is still allowed, but will be covered by the monojet searches at a 100 TeV  $pp$  collider [113].

## 5 Conclusion

In this work we have studied the prospect of current and future dark matter and collider experiments in probing the anomalous magnetic moment of the muon in the MSSM. By scanning the MSSM parameter space with the constraints of Higgs data, dark matter relic density, PandaX-II/LUX-2016 experiments and LHC-8 TeV searches for dilepton/triplet events, we found that the lightest neutralino  $m_{\tilde{\chi}_1^0} < 800 \text{ GeV}$  and the lightest chargino  $m_{\tilde{\chi}_1^\pm} < 940 \text{ GeV}$  is necessary to explain the anomalous  $(g-2)_\mu$  within  $2\sigma$  range. The combined Planck data and very recent PandaX-II/LUX data

largely rule out the MSSM parameter space favourable by  $(g-2)_\mu$  and by the dark matter relic abundance measurements within  $3\sigma$  range. We have also estimated the potential of a 100 TeV  $pp$  collider in covering the allowed parameter space and find that most of the parameter space with  $m_{\tilde{\chi}_1^0} < 710$  GeV and  $m_{\tilde{\chi}_1^\pm} < 940$  GeV (except for the compressed region) can be covered by searching for trilepton events.

**Acknowledgement.** This work was partially supported by the Australian Research Council. LW was also supported in part by the National Natural Science Foundation of China (NNSFC) under grants Nos. 11275057, 11305049, by Specialised Research Fund for the Doctoral Program of Higher Education under Grant No. 20134104120002.

## References

- [1] G. Aad *et al.* [ATLAS Collaboration], Phys. Lett. B **716**, 1 (2012).
- [2] S. Chatrchyan *et al.* [CMS Collaboration], Phys. Lett. B **716**, 30 (2012).
- [3] K. Hagiwara, A. D. Martin, D. Nomura and T. Teubner, Phys. Lett. B **557**, 69 (2003) doi:10.1016/S0370-2693(03)00138-2 [hep-ph/0209187].
- [4] F. Jegerlehner and A. Nyffeler, Phys. Rept. **477**, (2009) 1.
- [5] J. P. Miller, E. de Rafael, B. L. Roberts and D. Stöckinger, Ann. Rev. Nucl. Part. Sci. **62**, 237 (2012).
- [6] T. Blum, A. Denig, I. Logashenko, E. de Rafael, B. L. Roberts, T. Teubner and G. Venanzoni, arXiv:1311.2198 [hep-ph].
- [7] G. W. Bennett *et al.* [Muon g-2 Collaboration], Phys. Rev. D **73**, 072003 (2006).
- [8] M. Davier, A. Hoecker, B. Malaescu and Z. Zhang, Eur. Phys. J. C **71**, 1515 (2011) Erratum: [Eur. Phys. J. C **72**, 1874 (2012)].
- [9] K. Hagiwara, R. Liao, A. D. Martin, D. Nomura and T. Teubner, J. Phys. G **38**, 085003 (2011).
- [10] T. Aoyama, M. Hayakawa, T. Kinoshita and M. Nio, Phys. Rev. Lett. **109**, 111808 (2012).
- [11] C. Gnendiger, D. Stöckinger and H. Stöckinger-Kim, Phys. Rev. D **88**, 053005 (2013).
- [12] T. Aoyama, M. Hayakawa, T. Kinoshita and M. Nio, Phys. Rev. Lett. **109** 111808 (2012).

- [13] C. Gnendiger, D. Stöckinger and H. Stöckinger-Kim, Phys. Rev. D **88** 053005 (2013).
- [14] A. L. Kataev, Phys. Rev. D **86** 013010 (2012).
- [15] R. Lee, P. Marquard, A. V. Smirnov, V. A. Smirnov and M. Steinhauser, JHEP **1303** 162 (2013).
- [16] A. Kurz, T. Liu, P. Marquard and M. Steinhauser, Nucl. Phys. B **879**, 1 (2014).
- [17] A. Kurz, T. Liu, P. Marquard, A. V. Smirnov, V. A. Smirnov and M. Steinhauser, Phys. Rev. D **92**, no. 7, 073019 (2015).
- [18] F. Jegerlehner and R. Szafron, Eur. Phys. J. C **71**, 1632 (2011).
- [19] M. Benayoun, P. David, L. DelBuono and F. Jegerlehner, Eur. Phys. J. C **73** (2013) 2453.
- [20] A. Kurz, T. Liu, P. Marquard and M. Steinhauser, Phys. Lett. B **734**, 144 (2014).
- [21] G. Colangelo, M. Hoferichter, A. Nyffeler, M. Passera and P. Stoffer, Phys. Lett. B **735** 90, (2014).
- [22] G. Colangelo, M. Hoferichter, M. Procura and P. Stoffer, JHEP **1409**, 091 (2014).
- [23] G. Colangelo, M. Hoferichter, B. Kubis, M. Procura and P. Stoffer, Phys. Lett. B **738** 6, (2014).
- [24] G. Colangelo, M. Hoferichter, M. Procura and P. Stoffer, JHEP **1509**, 074 (2015).
- [25] V. Pauk and M. Vanderhaeghen, Phys. Rev. D **90** 11, 113012 (2014).
- [26] T. Blum, S. Chowdhury, M. Hayakawa and T. Izubuchi, Phys. Rev. Lett. **114**, no. 1, 012001 (2015).
- [27] L. Jin, T. Blum, N. Christ, M. Hayakawa, T. Izubuchi and C. Lehner, arXiv:1509.08372 [hep-lat].
- [28] G. Venanzoni [Fermilab E989 Collaboration], Nucl. Part. Phys. Proc. **273-275**, 584 (2016).
- [29] T. Moroi, Phys. Rev. D **53**, 6565 (1996) Erratum: [Phys. Rev. D **56**, 4424 (1997)].
- [30] A. Czarnecki and W. J. Marciano, Phys. Rev. D **64** (2001) 013014.
- [31] S. P. Martin and J. D. Wells, Phys. Rev. D **64**, 035003 (2001).
- [32] D. Stöckinger, J. Phys. G **34**, R45 (2007).

- [33] G. C. Cho, K. Hagiwara and M. Hayakawa, Phys. Lett. B **478**, 231 (2000).
- [34] G. C. Cho and K. Hagiwara, Phys. Lett. B **514**, 123 (2001).
- [35] K. Hagiwara, A. D. Martin, D. Nomura and T. Teubner, Phys. Lett. B **649**, 173 (2007).
- [36] G. -C. Cho, K. Hagiwara, Y. Matsumoto and D. Nomura, JHEP **1111**, 068 (2011).
- [37] M. Endo, K. Hamaguchi, S. Iwamoto and N. Yokozaki, Phys. Rev. D **84**, 075017 (2011).
- [38] M. Endo, K. Hamaguchi, S. Iwamoto, K. Nakayama and N. Yokozaki, Phys. Rev. D **85**, 095006 (2012).
- [39] M. Endo, K. Hamaguchi, S. Iwamoto and N. Yokozaki, Phys. Rev. D **85**, 095012 (2012).
- [40] M. Endo, K. Hamaguchi, S. Iwamoto and T. Yoshinaga, JHEP **1401**, 123 (2014).
- [41] M. Endo, K. Hamaguchi, T. Kitahara and T. Yoshinaga, JHEP **1311**, 013 (2013).
- [42] M. Endo, K. Hamaguchi, S. Iwamoto, T. Kitahara and T. Moroi, Phys. Lett. B **728**, 274 (2014).
- [43] J. L. Evans, M. Ibe, S. Shirai and T. T. Yanagida, Phys. Rev. D **85**, 095004 (2012).
- [44] G. Bhattacharyya, B. Bhattacharjee, T. T. Yanagida and N. Yokozaki, Phys. Lett. B **730**, 231 (2014).
- [45] M. Ibe, T. T. Yanagida and N. Yokozaki, JHEP **1308**, 067 (2013).
- [46] S. Akula and P. Nath, Phys. Rev. D **87**, no. 11, 115022 (2013).
- [47] S. Mohanty, S. Rao and D. P. Roy, JHEP **1309**, 027 (2013).
- [48] J. Kersten, J.-h. Park, D. Stöckinger and L. Velasco-Sevilla, JHEP **1408**, 118 (2014).
- [49] K. Kowalska, L. Roszkowski, E. M. Sessolo and A. J. Williams, arXiv:1503.08219 [hep-ph].
- [50] F. Wang, W. Wang, J. M. Yang and Y. Zhang, JHEP **1507**, 138 (2015).
- [51] F. Wang, W. Wang and J. M. Yang, JHEP **1506**, 079 (2015).
- [52] F. Wang, L. Wu, J. M. Yang and M. Zhang, Phys. Lett. B **759**, 191 (2016).

- [53] N. Okada, S. Raza and Q. Shafi, Phys. Rev. D **90**, no. 1, 015020 (2014) [arXiv:1307.0461 [hep-ph]].
- [54] I. Gogoladze, F. Nasir, Q. Shafi and C. S. Un, Phys. Rev. D **90** (2014) 3, 035008.
- [55] K. S. Babu, I. Gogoladze, Q. Shafi and C. S. Ün, Phys. Rev. D **90**, no. 11, 116002 (2014).
- [56] M. A. Ajaib, I. Gogoladze, Q. Shafi and C. S. Ün, JHEP **1405**, 079 (2014).
- [57] M. A. Ajaib, B. Dutta, T. Ghosh, I. Gogoladze and Q. Shafi, Phys. Rev. D **92**, no. 7, 075033 (2015).
- [58] M. Adeel Ajaib, I. Gogoladze and Q. Shafi, Phys. Rev. D **91**, no. 9, 095005 (2015).
- [59] I. Gogoladze, Q. Shafi and C. S. Ün, Phys. Rev. D **92**, no. 11, 115014 (2015).
- [60] M. Badziak, Z. Lalak, M. Lewicki, M. Olechowski and S. Pokorski, JHEP **1503** (2015) 003.
- [61] P. Athron *et al.*, Eur. Phys. J. C **76**, no. 2, 62 (2016).
- [62] G. Aad *et al.* [ATLAS Collaboration], JHEP **1310**, 130 (2013) Erratum: [JHEP **1401**, 109 (2014)].
- [63] S. Chatrchyan *et al.* [CMS Collaboration], JHEP **1406**, 055 (2014).
- [64] G. Aad *et al.* [ATLAS Collaboration], JHEP **1411**, 118 (2014).
- [65] S. Chatrchyan *et al.* [CMS Collaboration], Eur. Phys. J. C **73**, no. 12, 2677 (2013).
- [66] J. Fan, R. Krall, D. Pinner, M. Reece and J. T. Ruderman, JHEP **1607**, 016 (2016).
- [67] C. Han, K. i. Hikasa, L. Wu, J. M. Yang and Y. Zhang, JHEP **1310**, 216 (2013).
- [68] A. Kobakhidze, N. Liu, L. Wu, J. M. Yang and M. Zhang, Phys. Lett. B **755**, 76 (2016).
- [69] M. Drees and J. S. Kim, Phys. Rev. D **93**, no. 9, 095005 (2016).
- [70] The ATLAS collaboration [ATLAS Collaboration], ATLAS-CONF-2013-049.
- [71] V. Khachatryan *et al.* [CMS Collaboration], Eur. Phys. J. C **74**, no. 9, 3036 (2014).
- [72] G. Aad *et al.* [ATLAS Collaboration], JHEP **1404**, 169 (2014).

- [73] V. Khachatryan *et al.* [CMS Collaboration], Phys. Rev. D **90**, no. 9, 092007 (2014).
- [74] J. Ellis and K. A. Olive, Eur. Phys. J. C **72**, 2005 (2012).
- [75] H. Baer, V. Barger and A. Mustafayev, JHEP **1205**, 091 (2012).
- [76] G. Bélanger, G. Drieu La Rochelle, B. Dumont, R. M. Godbole, S. Kraml and S. Kulkarni, Phys. Lett. B **726**, 773 (2013).
- [77] M. Cahill-Rowley, R. Cotta, A. Drlica-Wagner, S. Funk, J. Hewett, A. Ismail, T. Rizzo and M. Wood, Phys. Rev. D **91**, no. 5, 055011 (2015).
- [78] J. Cao, Y. He, L. Shang, W. Su and Y. Zhang, JHEP **1603**, 207 (2016).
- [79] H. Fargnoli, C. Gnendiger, S. Paßehr, D. Stöckinger and H. Stöckinger-Kim, JHEP **1402**, 070 (2014).
- [80] S. Heinemeyer, W. Hollik and G. Weiglein, Comput. Phys. Commun. **124**, 76 (2000); Eur. Phys. J. C **9**, 343 (1999).
- [81] U. Chattopadhyay and A. Dey, JHEP **1411**, 161 (2014).
- [82] K. A. Olive *et al.* [Particle Data Group Collaboration], Chin. Phys. C **38**, 090001 (2014).
- [83] P. Bechtle *et al.*, Comput. Phys. Commun. **182**, 2605 (2011); Comput. Phys. Commun. **181**, 138 (2010).
- [84] L. Calibbi, J. M. Lindert, T. Ota and Y. Takanishi, JHEP **1411**, 106 (2014).
- [85] G. Belanger *et al.*, Comput. Phys. Commun. **182**, 842 (2011).
- [86] H. Baer, A. Lessa, S. Rajagopalan and W. Sreethawong, JCAP **1106** (2011) 031.
- [87] P. A. R. Ade *et al.* [Planck Collaboration], arXiv:1502.01589 [astro-ph.CO].
- [88] N. Arkani-Hamed, A. Delgado and G. F. Giudice, Nucl. Phys. B **741**, 108 (2006) doi:10.1016/j.nuclphysb.2006.02.010 [hep-ph/0601041].
- [89] D. S. Akerib *et al.* [LUX Collaboration], Phys. Rev. Lett. **112** (2014) 091303.
- [90] [http://pandax.physics.sjtu.edu.cn/files/pandax\\_ii\\_idm.pdf](http://pandax.physics.sjtu.edu.cn/files/pandax_ii_idm.pdf)
- [91] [http://luxdarkmatter.org/LUX\\_dark\\_matter/Talks\\_files/LUX\\_NewDarkMatterSearchResult\\_332L](http://luxdarkmatter.org/LUX_dark_matter/Talks_files/LUX_NewDarkMatterSearchResult_332L)
- [92] XENON1T Collaboration, E. Aprile, *et al.*, arXiv:1206.6288.
- [93] W. Porod, Comput. Phys. Commun. **153**, 275 (2003) doi:10.1016/S0010-4655(03)00222-4 [hep-ph/0301101].

- [94] J. Alwall *et al.*, JHEP **1407**, 079 (2014).
- [95] T. Sjostrand, S. Mrenna and P. Z. Skands, JHEP **0605**, 026 (2006).
- [96] J. de Favereau, *et al.*, arXiv:1307.6346 [hep-ex].
- [97] M. Cacciari, G. P. Salam and G. Soyez, Eur. Phys. J. C **72**, 1896 (2012) [arXiv:1111.6097 [hep-ph]].
- [98] M. Cacciari, G. P. Salam and G. Soyez, JHEP **0804**, 063 (2008).
- [99] CMS-PAS-SUS-16-024.
- [100] M. Drees *et al.*, Comput. Phys. Commun. **187**, 227 (2014).
- [101] W. Beenakker, R. Hopker and M. Spira, hep-ph/9611232.
- [102] A. Barr and J. Scoville, JHEP **1504**, 147 (2015).
- [103] P. Schwaller and J. Zurita, JHEP **1403**, 060 (2014).
- [104] C. Han, A. Kobakhidze, N. Liu, A. Saavedra, L. Wu and J. M. Yang, JHEP **1402**, 049 (2014).
- [105] H. Baer, A. Mustafayev and X. Tata, Phys. Rev. D **89**, no. 5, 055007 (2014).
- [106] C. Han, L. Wu, J. M. Yang, M. Zhang and Y. Zhang, Phys. Rev. D **91**, 055030 (2015).
- [107] B. Dutta *et al.*, Phys. Rev. D **91**, no. 5, 055025 (2015).
- [108] B. Dutta *et al.*, Phys. Rev. D **90**, no. 9, 095022 (2014).
- [109] N. Arkani-Hamed, T. Han, M. Mangano and L. T. Wang, arXiv:1511.06495 [hep-ph].
- [110] T. Cohen, T. Golling, M. Hance, A. Henrichs, K. Howe, J. Loyal, S. Padhi and J. G. Wacker, JHEP **1404**, 117 (2014).
- [111] S. Gori, S. Jung, L. T. Wang and J. D. Wells, JHEP **1412**, 108 (2014).
- [112] B. S. Acharya, K. Bożek, C. Pongkitivanichkul and K. Sakurai, JHEP **1502**, 181 (2015).
- [113] M. Low and L. T. Wang, JHEP **1408**, 161 (2014).
- [114] S. A. R. Ellis and B. Zheng, Phys. Rev. D **92**, no. 7, 075034 (2015).
- [115] J. L. Feng, S. Iwamoto, Y. Shadmi and S. Tarem, JHEP **1512**, 166 (2015).